Human Identity Verification From Biometric Dorsal Hand Vein Images Using the DL-GAN Method

KHALED MOHAMED ALASHIK AND REMZI YILDIRIM

Department of Computer Engineering, Ankara Yildirim Beyazit University, 06760 Ankara, Turkey

Corresponding author: Khaled Mohamed Alashik (k_elashek@yahoo.com)

ABSTRACT In this research, biometric authentication, which has been widely used for different purposes in the last quarter-century, is studied. Dorsal hand veins are used for biometric authentication. ''Deep learning'' (DL) and ''generative adversarial networks'' (GANs) are used together as keys in the study. A DL-GAN is obtained by combining deep learning and GAN. The developed DL-GAN method is tested on two separate databases. The adversarial network (DL-GAN) method is developed to increase the authentication process's proportional value. For identity verification, dorsal hand veins with biometric physical properties are used. A multistep approach is used for selecting hand dorsal features, including preimage processing and effectively identifying individuals. The deep learning productive antinetwork method is used to effectively identify individuals based on the information obtained from the dorsal hand vein images. For the test in the study, two open access databases are used. These databases are the Jilin University - dorsal hand vein database and the 11K hands database. The results of the experiments performed on the dataset related to the dorsal hand vessels show that the DL-GAN method reaches an identity accuracy level of 98.36% and has an error rate of 2.47% and a standard accuracy of 0.19%. The accuracy of the experimental results in the second dataset is 96.43%, the equal error rate is 3.55% and the standard accuracy is 0.21%. The improved DL-GAN method obtains better results than physical biometric methods such as LBP, LPQ, GABOR, FGM, BGM and SIFT.

INDEX TERMS Security, identification, biometrics, detection system, hand veins, deep learning, generative adversarial network.

I. INTRODUCTION

In today's world, the individual authentication process is widely used for security purposes. This identity verification technique is considered an innovation brought by modern technology. This innovation uses many different techniques and methods to verify identity to increase security in many areas. Among these different techniques, the biometric authentication technique is the most popular and used worldwide. It is an authentication process using personal biometric properties. The commonly used person physical biometric measurements are fingerprints [1], irises [2], palm prints [3], faces [4], speech [5], retinas [6], and palm print-based systems [7] for identification. There are also nonphysical or behavioral biometric properties, such as handwriting, psychological conditions, DNA, and gait.

Biometric methods can be based on a person's face, but the accuracy of these face recognition methods depends on the state, gesture, and brightness of the image. In biometric methods based on face image processing, many factors play a role. We can mention the feeling inside the image, the person's age, the quality of ambient light, and the imaging angle [8].

Another important biometric method is the classical use of fingerprints, but these methods have challenges. For example, the fingerprints of elderly people or people such as workers are difficult to recognize. Hard work and physical activity in some occupations cause people to lose their fingerprints, and identifying them with these methods is challenging [9]. In some cases, people intentionally destroy their fingerprints temporarily or permanently with acid or burns to make them difficult to identify in criminal activities [10].

The associate editor coordinating the review of this manuscript and approving it for publication was Haruna Chiroma.

An appropriate method for identifying people is to use iris information. The iris authentication method has high accuracy, but unfortunately, it faces challenges. Iris biometric detection requires specific cameras, hardware, and substrates necessary for this method and has made its use costly [11]. Palm line information is one of the most widely used methods of identifying individuals. Studies show that the groove pattern and even the hand arteries can be unique and identify individuals with great accuracy. This method can use tissue features such as wrinkles, bumps, and the human palm folds for identification [12], [13]. Different palm printing features, such as geometric features, lines, and wrinkles in other people, have different and unique patterns. These methods can be used in biometrics and individual identification. Palm prints have various features in terms of vascular location and fingerprints and a set of features that can be used for identification. To analyze hand images, blood vessels can be used, and fingerprints or hand grooves can be used in printing [14], [15].

Fingerprint recognition or hand printing has been considered in many security applications. Compared to other human physiological features, fingerprints and palm prints are important factors in identifying individuals.

Most studies focus on texture-based, line-based, subspace learning-based, correlation filter-based, local descriptor-based, and orientation coding-based methods [16]. Palm scratch information can be affected and unusable in some hard workers, such as workers and miners. Information on the palm's grooves can be subject to change or tissue damage, but the pattern of the arteries in the hand has a very stable pattern. The veins in the hand consist of two parts, the back and the palm. Using patterns of arteries and veins on the hand's back is a sure method of identification and cannot be forged [17]. The palm veins are more difficult to distinguish from the back of the hand because the palm has denser tissues than the back of the hand. An appropriate method for detecting hand veins is to use infrared cameras. With these cameras, one can then make contact with a certain surface and read the pattern of the hand's veins. The advantage of this identification method is that unlike manual printing methods, the person does not need to contact the surfaces.

II. HAND BIOMETRIC

Many features are used for security hand biometric authentication. Its use has been widely preferred in recent years due to its effective authentication feature and its accuracy [18]–[22]. One of the biometric features of the human hand is palm lines and vein marks. It is used in authentication for security purposes and biometric identities because it is difficult to replicate personalized avatar traces and vessels [23]–[26].

Apart from hand properties, there are other important biometric properties. One of them is dorsal hand veins [27]–[29] and palm veins [30], [31], and hand vein biometry and authentication are also used in many parts of daily life. The main areas of use are airports, banking systems and everywhere where security is high. This new biometric technique is safer

than other conventional biometric techniques. New biometric techniques brought by technology are also becoming widespread with new techniques daily. The main of these is hyperspectral technology [32]–[35]. By combining the hyperspectral mode and technology with the biometric features of the other hand, higher security identification systems can be obtained [36], [37].

The hyperspectral method or technique uses spectral information on a biometric hand image. This additional spectral information includes the dermal skin layers, epidermal layers, absorption coefficient, and hemoglobin. Thus, the reliability of identification is increased [36]. It is challenging to change and imitate the information obtained depending on the skin [37]. Specific knowledge, which is linked to that person's skin, can be obtained using infrared and thermal cameras [38]. The spectral information obtained is used as a supplement to the hyperspectral information. The advantage of this is that it increases the accuracy rate in obtaining the person's biometric properties and correctly determining identity.

The hyperspectral technique, which has a high-reliability feature, has two types: single spectral and multispectral. For a single spectrum palm, Fei *et al.* [39] and Zhang *et al.* used multispectral data [40], as did Hong *et al.* [41]. Huang *et al.* [29] performed adorsal hand vessel studies [42]–[44], and Chuang [45] used hyperspectral techniques to improve dorsal hand biometry.

Other studies include hand biometric measurements in tissue analysis [46], [47], Liu *et al.* [48], palm scar lines, Wu *et al.* [49] proposed the CompCode (competitive code) technique, and Xu developed it into CompCode [50]. For the dorsal hand vein, Xu *et al.* [51] used LBP for the local SIFT and the dorsal hand vein according to the Gabor filter by Wang *et al.* [52] and designed filter banks to recognize the dorsal hand vein.

The refraction factor is significant for improving biometric hand image quality [53]–[55]. It is essential that the cameras used to obtain high-quality biometric hand images are of high quality and have good calibration [56]. Wang and Wang [57] also found that biometric hand edge background lines effectively determine biomechanical hand features.

A. RELATED WORKS

In the literature, dorsal vein detection methods generally follow similar procedures such as preprocessing, feature extraction, and similarity measurement. These methods can be roughly divided into two groups according to their characteristics of showing vascular patterns: shape and texture. The first type focuses on shape features derived from the structural composition of the hand vein network to identify individuals. In some studies and early searches, the positions and angles of short straight vectors [58] and small points [59]–[61] are used to describe the distinction between vessel shapes, including endpoints and intersections. Zhu and Huang [62] proposed a graphical representation of the vessel shape for recognition, which simultaneously encodes both the

resemblance of information and line segments with a single model. For the latter, as a function to discern various persons, region of interest (ROI) text is extracted from the vein image. Textures may be used in the initial analysis of both main components (PCA) [63] and linear discriminant analysis over the whole image (LDA) [64] and local binary models (LBP) [65] and scale-invariant feature transform (SIFT) in certain areas [66]–[68]. These methods described above can also be categorized on a general and local basis in terms of how to extract the functions. To assess similarity, systematic methods use tissue or shape details of the dorsal artery as a whole, and PCA [64], LDA [63], and graph [62], [69]-based methods belong to this pattern. However, they seem to be susceptible to changes in light, distortion, and obstacles that induce output degradation. Local elements that remove texture or form, including LBP and SIFT, features in a particular area are more resistant to these factors and dominate such a problem.

Coding methods also attempt to encode and encrypt image information, and examples of these methods are the use of wavelet and GABOR filters. Hybrid approaches use two or more methods. Combined methods use the various benefits of authentication methods. D. Huang, X. Zhu, Y. Wang, and D. Zhang [70] presented a fractal dimension box-counting method for identification based on the pattern of venous vessels. In biometric systems, feature extraction from images is regarded as the most important step. Their experimental studies, based on data from the Bosphorous dorsal venous database, indicate that, relative to other known methods, their proposed approach has positive and encouraging outcomes. The advantage of this method is the use of a back structure for authentication, which increases its accuracy, and the main challenge of this method is the high complexity of the method. Y. Aberni, L. Boubchir, and B. Daachi [71] presented palm vein recognition based on a competitive coding scheme using a multiscale local binary pattern with ant colony optimization (ACO). The ant colony algorithm in their method allows possible blocking points related to image quality or contrast problems that can be seen with images from the near-infrared spectrum to be ignored. Images are then preprocessed and sorted using the MLBP method by a competitive coding program. Experimental results obtained in the MS-PolyU database have shown that the proposed method has high accuracy in identifying individuals. O. Alpar [72] proposed a new fuzzy curvature method for detecting hand veins by thermal imaging. In their method, first, the arm image taken by a thermal camera is divided into two parts and filtered by a Gaussian high-pass filter to smooth and enhance the contrast. The fusion method by the fuzzy inference system as an expert system can be expressed as the main topic in infrared thermal imaging. Despite the high accuracy of this method, their proposed mechanism requires special hardware, and its implementation cost is high. In F. Liu, S. Jiang, B. Kang, and T. Hou [73], a recognition system for partially occluded dorsal hand veins using improved biometric graph matching was presented. An important advantage

of this method is that some of the dorsal parts may be lost due to damage, pigmentation, or tattooing and affect the identity of individuals. In this method, they are reconstructed. Their experimental results have shown that the error rate and accuracy of this method are desirable, and if a person uses tattoos, this method can identify the person. In A. Achban, H. A. Nugroho, and P. Nugroho [74], wrist hand vein recognition using a local line binary pattern (LLBP) was used to identify an individual based on hand vein information. This study tries to use the local line binary pattern method in the feature extraction stage. In this study, the data of 50 individual datasets taken directly with infrared cameras were used. Their experiments showed that the accuracy of this method is approximately 96.50%. H. Qin, M. A. El Yacoubi, J. Lin, and B. Liu [75] presented an iterative deep neural network for hand vein verification. This paper proposed an iterative deep belief network (DBN) for deriving vessel characteristics based on primary tag data. Samples were generated automatically using very limited prior knowledge and are repeatedly modified by DBN. The resulting venous features were used to reconstruct the training dataset, according to which the network was retrained. Experimental results in two general databases showed that their proposed method is effective, but its accuracy depends heavily on prototypes for training. R. Garcia-Martin and R. Sanchez-Reillo [67] presented vein biometric recognition on a smartphone. In R. S. Kuzu, E. Piciucco, E. Maiorana, and P. Campisi [77], on-the-fly finger vein-based biometric recognition using deep neural networks was introduced. They introduced a deep learning architecture capable of capturing the structure of a finger vein using a set of low-cost cameras. In this study, a diagnostic framework using convolutional neural networks was proposed. Experimental results showed that the accuracy of this method is high, but an important challenge is the need to use additional cameras to implement the design.

For feature extraction, there are two categories: texture-based and shape-based [69], [78]. The first category uses tissue changes and tissue statistical characteristics for identification. For example, Li and Kang introduced several improved local binary pattern (LBP) models to define the characteristics of ship models [79], [81]. Premalatha and Kumar examined local phase quantization (LPQ) and its alternatives to determine an identifier for individual identification [82], [83]. Wei used hyperspectral images of the dorsal hand vein to extract discriminative local features [84]. The improved model of the scale-invariant feature transform (SIFT) method was implemented by Wang for use in cross-device hand vein recognition [85]. To minimize the rotation and effects of noise and shifting problems and to maximize the discriminatory power of feature extraction, Meng and Wang used the Gabor filter and its variants [86], [87]. In general, algorithms related to texture-based feature extraction focus on texture changes but do not consider the overall geometric shape of the ship model, therefore leaving an area for improvement in detection accuracy [69]. Feature extraction based on tissue is not a fundamental

distinction between individuals and is not strong for changes in lighting conditions [78].

Deep learning is a field of study that includes neural networks and similar machine learning algorithms with one or more hidden layers. In other words, it is the use of at least one artificial neural network (ANN), and the computer obtains new data from the available data with many algorithms. Supervised, semisupervised or unsupervised deep learning should be carried out. Deep artificial neural networks have also yielded successful results with a reinforcement learning approach [89]. Deep learning allows computational models consisting of multiple processing layers to learn to display data with multiple levels of abstraction. This technology has dramatically improved the most advanced technology in many other areas, such as speech recognition, visual object detection, object detection, and drug and genomic detection. In-depth learning using the reverse diffusion algorithm examines the complex structure in a large dataset to determine how a machine should change its internal parameters used to calculate the display in each layer of the display in the previous layer. Deep convolutional networks have revolutionized the processing of images, videos, speech, and audio, while recurring networks illuminate sequential data such as text and speech [89]–[91].

Although deep learning methods generally surpass traditional handmade methods for biometric detection, there are some technical problems and obvious issues, including the availability of high-quality labeled training samples, high computational cost, high storage, hardware needs, poor portability, and a complex design model. Therefore, attempting to solve the challenges mentioned above forms the future process of deep learning. Many new types of machine learning problems, such as uncontrolled, semisupervised and self-supervised learning, have been explored to reduce dependence on labeled learning items. Compression technologies such as pruning, quantization and data distillation are used to reduce computational/storage costs. Lightweight deep learning models such as MobileNet and ShuffleNet are built for mobile environments or to increase portability. Additionally, many researchers are attempting to improve the interpretability of deep learning models. In summary, deep learning technologies with their rapid development will certainly play an important role in biometric cognition [88].

The deep learning method is only one of the methods and successes developed based on computer systems with a recent history [93]. This technique allows the abstraction of more than one data point. It also consists of more than one computational model and layer. This method is used in many different areas including translation, voice, speech, visual object recognition and perception. In short, biometric identification is also widely used in the field. In addition to these, it is also used in research fields such as medicine and genes in industry [92]. By using the advantages of deep learning techniques, the method extracts and completes the features sought in studies conducted in accordance with the purpose. Because of this feature, it can be used widely in
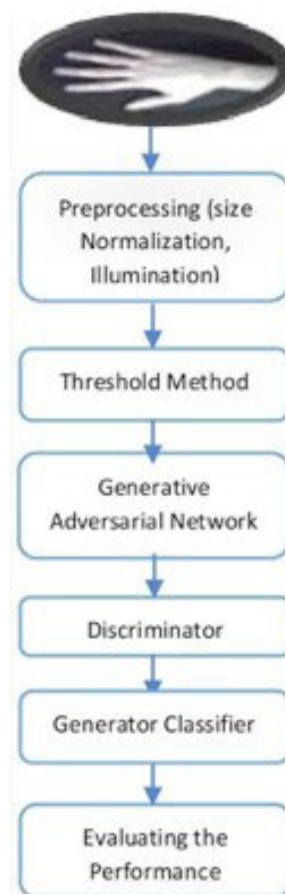

FIGURE 1. Overall block systems of the proposed method.

biometric applications and industry. In addition, it provides a great advantage to users due to its natural language processing and recognition features. [91]. Deep learning is widely used in biometrics. Its use in this area brings great advantages. Although the deep learning method performs well over other methods, it has some disadvantages. The main disadvantages are higher education human resources or qualified people, calculation and storage cost expenses, hardware needs of the computers used, portability and complexity. These problems constitute the problems that deep learning should solve in the future [89]. Deep learning models have been used extensively in electronic systems for security purposes in recent years. The main systems are phone, computer, authentication and security. [92]. Because the size of neural networks is critical, deep learning requires high-performance hardware and software infrastructure. Deep learning usage areas, positive aspects and negative aspects are given in the resource. [94], [95].

The biometric authentication method is more reliable and easier than other methods [92]. It offers an end-to-end learning paradigm for combining deep learning, feature extraction and preprocessing and recognition based solely on biometric data [93]. Among the main advantages of deep learning is a strong learning ability, broad scope, adaptability, data-driven nature, good transferability, etc.
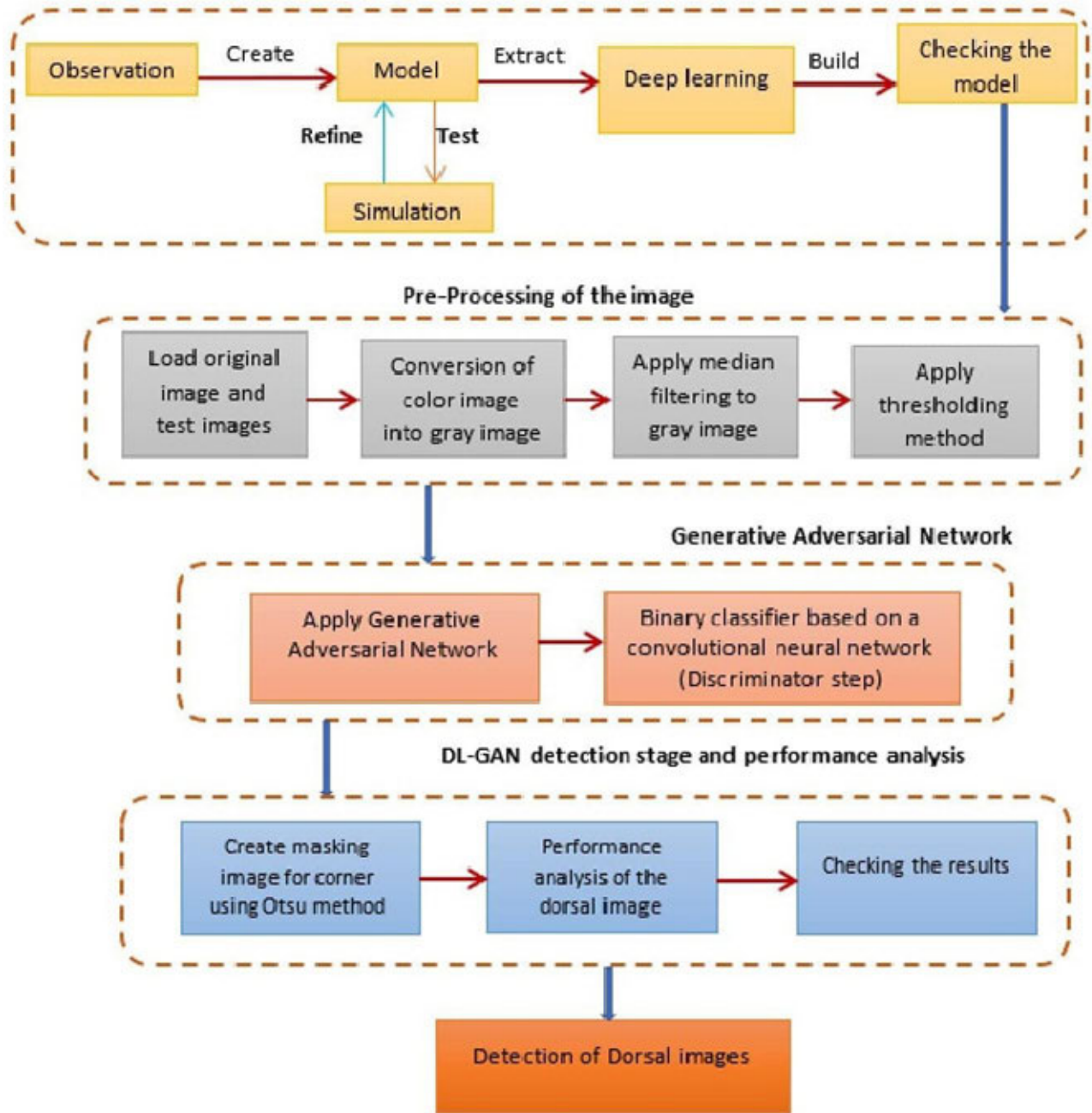
FIGURE 2. DL-GAN network for identification based on hand dorsal veins.

In this study, the technological advantages of the deep learning method were used for authentication. These advantages are automatic pattern fit features and provide an estimate of the density function. GAN is the newer model of the deep learning family. In the application, using this deep learning feature will be compared with the applications in two databases. Detailed specifications of Jill University and the 11K database were written. The experiments are illustrated on the Jilin University - dorsal hand vein database (Table-1) and the 11K hands dataset (Table-2), the most comprehensive databases, and comparative results are achieved, which shows

the advantage of deep generative adversarial network features over light features in dorsal hand vein recognition.

III. DL-GAN METHOD

In this article, a biometric method based on venous processing is presented to identify individuals. The proposed method uses GAN-based deep forging technology to identify individuals, as shown in Figure 2. In this article, we propose a productive model for identifying individuals based on the identification of the veins, which is explained in the following method and its components.

As shown in Figure 1, in this paper, there are seven steps: reading the image, preprocessing, applying the threshold method, generative adversarial networks, discriminators, generator classifiers, and evaluation of the performance. All these steps are explained in the following steps.

The framework of the proposed method for authentication using hand vein information is shown in Figure 2.

FIGURE 3. Display of dorsal hand veins in the back of the hand with infrared camera s.

A. INPUT IMAGES

One method for obtaining input images is to use high-resolution IVYRISE cameras, which can be downloaded from Amazon at a reasonable price. Figure 3 shows a view of these infrared cameras to show the veins of people's hands in the image on the left. The images on the right show an example of the veins in the dorsal hand vein of people after the initial preprocessing. Another method is to use training and test datasets; in this paper, we used the Jilin University - dorsal hand vein database.

B. PREPROCESSING IMAGES

Infrared images of people's hands are created based on the sensitivity of these cameras to hemoglobin. The output images of this method can be of good quality. However, in generating these images, handshake or ambient noise can impair the image quality. Therefore, it is necessary to perform preprocessing on the images before deep learning. In the proposed method, the images are first converted to gray with a light intensity between 0 and 255, and then a median The noise filter calculates the midpoints of a neighborhood of light intensity to eliminate noise, and Eq (16) suggests [96] noise f:

$$f = \underset{(i,j) \in K}{median}\{H(i,j)\} \tag{1}$$

where K is the number of adjacent and neighboring pixels of a central pixel. H is accompanied by the noise of a hand image. f is the same as the image after the median filter. Automatic vein authentication requires preprocessing of images. If the image quality is enhanced before authentication, the accuracy of the authentication can be ensured. One of the main methods to increase the quality of images is to use the histogram chart balancing technique. To represent the conversion function s = T (r) to balance the image, Equation (17), which is an integral, can be used:

$$s = T(r) = (L - 1) \int_0^r P_r(w)dw \tag{2}$$

where L is the highest level of light intensity in the image, and this value is 256 in gray images. This relation can be considered for the discrete state and can be represented as Eq (3):

$$S_k = T(r_k) = (L - 1) \sum_{j=0}^{k} p_r(r_j)$$

$$= \frac{(L - 1)}{MN} \sum_{j=0}^{k} n_j \quad k = 0, 1, 2, \ldots, L - 1 \tag{3}$$

where MN is the total number of pixels in the image. n_k is the number of pixels with light intensity r_k. L is the number of levels of brightness used in the image. In the next step, after initial preprocessing and graying of the images, it is necessary to consider an input image, where their size is normalized to 256 by 256. In the second phase, according to the diagram in Figure 4, with edge detection methods such as Prewitt and Sobel, the edge and the image area of the individual's hand can be extracted, and this area of interest can be considered for further processing.

FIGURE 4. From left to right, the gray image of the hand and its veins, the image of the edge and our area of interest with Sobel edge, the extraction of the segmentation of interest or ROC by filling the cavities, the extraction of the veins of the hand, respectively.

The following steps can be used to extract areas of interest in the hand and identify the pattern of veins:
- Capture frames: One hand needs to be inserted into the device for a few seconds, and then cameras at 34 to 36 frames can capture still images.
- ROI extraction: In this step, the image and the desired section can be extracted by hand. Some methods use a circular section for extraction, but these methods are not very effective because some important recognition vessels are located in the finger. The proposed method uses gradient-based edge detection, such as Sobel, to edge the image areas. In the proposed method, small areas can be removed from the image by thresholding the size of the hand area and filling the image holes.
- Extraction of hand veins: Image thresholding methods can be used to extract hand veins as input to deep learning techniques. By image thresholding, hand veins can be detected and binary and used as a learning model in deep forging or GAN networks.

C. THRESHOLD METHOD

The Otsu thresholding method uses a procedure based on statistical processes to find the optimal thresholds.

In this technique, the difference between the mean and variance in light intensity on both sides of the thresholds is used to find the optimal values for them. Otsu thresholding is a definite method of determining thresholds. In this algorithm, an attempt is made to maximize the amount of variance in light intensity on both sides of the thresholds. To model the proposed method, it is assumed that p_i is equal to the frequency of the number of pixels that have a light intensity of i and can be calculated according to Equation (19) [97]:

$$p_i = \frac{n_i}{N}, \quad p_i \geq 0, \quad \sum_{i=0}^{L} p_i = 1 \quad (4)$$

where ni is the number of pixels in the whole image that has a light intensity equal to i and N is the total number of pixels in the image. L is the light intensity that here is selected as 255. In the simplest case, assume that there is only one threshold such as t in the image, and this threshold in the histogram can set the light intensity 0 to t-1 on its left. Light intensity t to L is also on its right, and here in gray images. In Otsu thresholding, the total weight or frequency of the two classes to the left and right of threshold t can be calculated as Equations (5) and (6), respectively. The sum of these two weights to the right and left of the classes, as Equation (7), is equal to one [97]:

$$w_0 = \sum_{i=0}^{t-1} p_i \quad (5)$$

$$w_1 = \sum_{i=t}^{L-1} p_i \quad (6)$$

$$w_0 + w_1 = 1 \quad (7)$$

where w_0 and w_1 are weighted classes for the left and right sides. In the next phase, the weighted average light intensity of the left and right sides of the threshold is calculated according to Equations (8) and (9). This mechanism can be used to calculate the average of the two classes of left and right thresholds, which is shown in Equation (10). Using the weights of the two classes and the calculated average, such as Equation (11), it is possible to define an appropriate objective function whose goal is to maximize the optimal threshold [56]:

$$\mu_0 = \sum_{i=0}^{t-1} \frac{i.p_i}{w_0} \quad (8)$$

$$\mu_1 = \sum_{i=t}^{L-1} \frac{i.p_i}{w_1} \quad (9)$$

$$\mu_T = w_0\mu_0 + w_1\mu_1 \quad (10)$$

$$f = w_0.(\mu_0 - \mu_T)^2 + w_1.(\mu_1 - \mu_T)^2 \quad (11)$$

where μ_0 and μ_1 are the weighted average light intensities in the pixels of the two classes to the left and right of the threshold, respectively, μ_T is the weighted average light intensity of the two sides of the threshold and f is the objective function. If several thresholds such as the m threshold are used, the objective function can be presented as a general Equation (12) [97]:

$$f = w_0.(\mu_0 - \mu_T)^2 + w_1.(\mu_1 - \mu_T)^2 \\ + \cdots + w_m.(\mu_m - \mu_T)^2 \quad (12)$$

Here, the goal is to find the optimal threshold $T^* = (t_1, t_2, \ldots, t_m)^*$ to maximize the value of the objective function, and these thresholds are suitable for segmentation.

D. GENERATIVE ADVERSARIAL NETWORK (GAN)

Generative adversarial networks (GANs) have two networks, generators, and splitters. GAN is the ultimate advanced learning model [97]. Goodfellow, *et al.* 2014 developed some algorithms for artificial intelligence [94]. These include GAN networks. GAN networks are a group of algorithms for unsupervised learning. The advantage of this is that they produce near-real images using the basis of game theory and a zero-output model scenario. Despite significant achievements to date, the use of GANs for real-world problems still poses significant challenges for all three, which we focus on here. These include (1) creating high-quality images, (2) providing diverse, and (3) sustainable training. However, GANs are not without problems. Most importantly, they are difficult to train and difficult to evaluate. Given the difficulty of training, maintaining a balance between the differentiator and the product during training is not trivial, and it is usually normal for the producer to learn well, that is, to fully distribute the dataset [95].

In recent years, deep learning methods with the generative adversarial network (GAN) approach have become a convenient tool for pattern recognition and have high accuracy. The contribution of this paper is using a multistep approach including feature selection and image preprocessing along with the GAN method to effectively identify individuals based on information from dorsal hand vein images. Biometrics-based identity verification research was performed, and the DL-GAN method was developed and tested in the same databases in different ways. The results obtained from the DL-GAN were verified by different methods under the same conditions obtained and the results of the comparison. while an approach that could create a large number of educational and artificial examples is the application of DL-GAN. One of the areas of GAN learning is the use of this method of image processing.

The experimental results show the advantage of deep generative adversarial network features over light features to discriminate dorsal hand vein networks and confirm the inevitability of the fine-tuning step.

Generative adversarial networks (GANs), first proposed by Goodfellow *et al.* in 2014, provide improvements to sequence generation in the context of representation of input features within a complete body of work [98]. When faced

with generating photo quality images of real-world objects, LSTM RNNs will recall patterns and track position within a generated sequence but exhibit the potential to overcompensate; there appears to be a limit to their ability to construct a complete work on their own. The proposed solution in Goodfellow's paper adds an additional level of scrutiny to the LSTM RNN's sequence generation, an RNN-based model trained to critique predicted output [98]. This provides the adversarial nature alluded to in the GAN naming convention, which amounts to two NNs trained on the same data. The generative adversarial network shown in Figure 5 consists of two separate neural networks. One network is abbreviated G, meaning generator, and the other network is abbreviated D, which means differentiator. The G network first produces random images. Network D examines the images and tells G how similar the images are to the actual image [30].
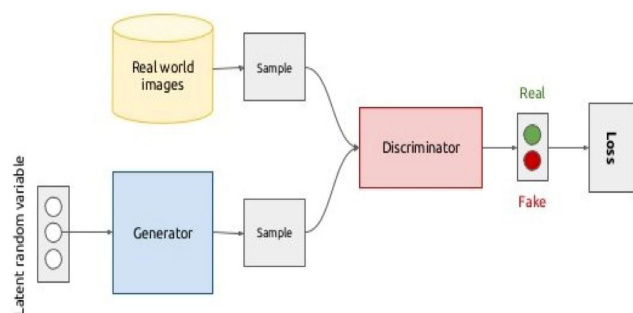

FIGURE 5. Learning in the generative adversarial network.

In the initial phase, a generating model takes random noise signals as input and produces a distorted image as output. Gradually, with the help of the D network, it creates images of the desired class that look real. The distinctive network, which acts as a competitor to the generating network, takes the generated images of the generating network along with a specific class of real images as input and then evaluates how much the generated images are evaluated with the real image. After going through several stages of network operation, we reach a point where the differentiating network cannot recognize whether the images produced are real. This is the point at which the generating network produces images of a specific class (the class with which network D is trained) that did not exist before. Deep learning is like giving a picture of a hand to a thief. In the second step, you check this image with your hand image and if the similarity is not confirmed, the image will be given to the forger again and the forger will apply some noise to it and change it slightly to increase the level of adaptation with your image. This process of moving the image of the hand between you and the forger goes so far that the fake image is slightly different from the real image. In the proposed method, training is performed at two levels. The dorsal hand veins are noisy and then matched to the original image to select an image that produces fewer matching errors. In the proposed method, deep learning for biometric training and adaptation is performed using GAN. Generative adversarial networks have been very successful

in deep learning and image processing, and in these networks, high accuracy can be achieved by increasing the size of the training data. One of the limitations of many deep learning methods is that they require considerable training data to achieve high accuracy. In most cases, there are not enough training samples available. For example, data related to the effect of manual veins may be limited, and therefore, the chances of increasing accuracy in biometrics will decrease as the number of training samples decreases. The advantage of a learning GAN is that it can generate a large number of random instances with game theory. Classifiers, such as convolutional neural networks, usually require a large dataset for training. The GAN method has the advantage that it can create a large number of artificial samples for training to increase its accuracy, which will increase the power of this method for image classification. We present a method to use these hostile networks, and we want to estimate whether these artificial examples added to the main training database images can improve the accuracy of the test database.

Class imbalance is a major issue when training deep learning algorithms to perform classification tasks on biometric images. A common technique to address the class imbalance in training data is to geometrically augment existing images. Data augmentation is the use of geometric and other transformations to create new images from existing images. It has been a proven technique for improving the generalizability of deep learning models. However, the optimal methods for augmenting training images are often unknown to researchers before training; hence, extensive tuning is needed. Moreover, the number of methods for augmenting a given image is limited, and it is impossible to create unlimited numbers of images simply using data augmentation.

This led to the invention of generative adversarial networks (GANs) [98]. GANs have recently received much attention due to their ability to synthesize realistic images from white noise vectors. The originally proposed GAN architecture consists of two dCNNs competing against each other. Figure 6 shows the architecture of a GAN in the most general sense:
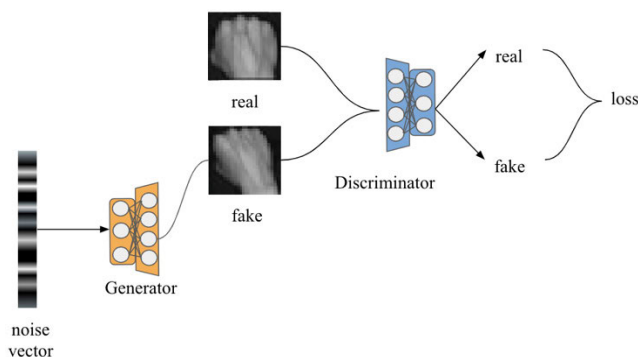

FIGURE 6. GAN architecture. A 'fake' image is generated by the generator from a random noise vector. The discriminator is tasked with classifying 'fake' images from real training data.

In Figure 6, the two competing dCNNs are a generator network that generates synthetic images from noise and a discriminator network that discriminates real samples from

fake ones. A common learning objective of GANs is for the generator to 'fool' the discriminator with fake images that increasingly become realistic. Mathematically, we can express this learning objective as a minimax loss:

$$\min_G \max_D V(D, G) = E_{x \sim P_{data}(x)}[\log D_x] \\ + E_{zP_z(z)}[\log(1 - D(G(z)))] \quad (13)$$

where x and z are the inputs for the discriminator. In Equation 13, the training objective of the discriminator (denoted as D) is to maximize $\log(D(x)) + \log(1 - D(G(z)))$, the probability of assigning correct labels to both training images and synthetic (or 'fake') images generated by the generator network G. The generator is trained to minimize $\log(1 - D(G(z)))$, the inverted log probability of the discriminator's prediction of fake images. Minimization of the inverted probability is hard to implement, and therefore, we seek to maximize D(G(z)) instead.

The original GAN can synthesize realistic images. However, it can only randomly synthesize them and is often susceptible to mode collapse. Mode collapse occurs when the generator decides to select the 'easiest' class in the dataset to successfully fool the discriminator. The resulting images lack diversity, and usually, they all belong to the same class. In practice, mode collapse occurs very often due to class imbalance in training data. One method for addressing mode collapse and correcting the problems appearing in unconditional image synthesis is to incorporate side information. Conditional GAN (cGAN) is a common type of GAN that uses a generator that conditionally generates images based on class labels [102]. The auxiliary classifier GAN (ACGAN) is a type of cGAN that uses an additional auxiliary classifier to assign the correct class labels to synthesized images [100]. Figure 7 shows the general architecture of ACGAN:
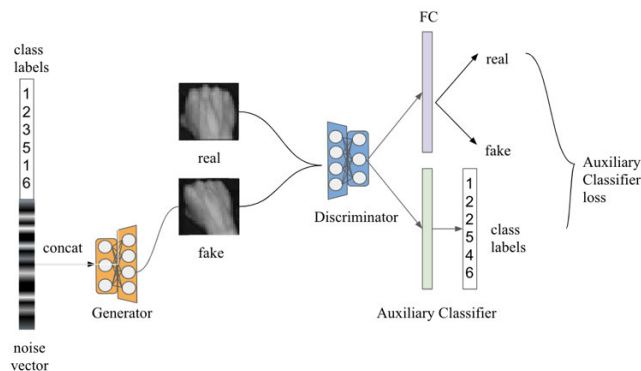

FIGURE 7. ACGAN architecture.

ACGAN uses additional class labels during image synthesis to not only conditionally synthesize images but also to improve the quality of the synthesized images.

Since ACGAN includes an additional auxiliary classifier in its discriminator, its objection functions are defined as follows:

$$L_s = E[\log P(S = real | X_{real})] + E[\log P(S = fake | X_{fake})] \quad (14)$$

$$L_s = E[\log P(C = c | X_{real})] + E[\log P(C = c | X_{fake})] \quad (15)$$

defined. In addition to producing a probability distribution P(S|X) = D(X) over possible image sources, ACGAN's discriminator also contains an auxiliary classifier that produces a probability distribution P(C|X) = D(X) over the class labels of the images. Objective functions 14 and 15 are defined as the loglikelihood of the correct image source LS and the loglikelihood of the correct class LC.

Pix2pix is a popular variant of cGAN that is commonly used in image-to-image translation tasks. It is built upon the well-known segmentation network UNet and uses adversarial learning to achieve modality transfer. In pix2pix, the generator is usually a UNet (or any other encoder-decoder network), and the discriminator is a convolutional "PatchGAN" classifier. Unlike other cGANs, pix2pix uses a dual objective function that combines adversarial loss with L1 loss:

$$G^* = \arg \min_G \max_D L_{cGAN}(G, D) + \lambda L1 \quad (16)$$

E. DISCRIMINATOR

The discriminator in deep forging is a binary classifier in which inputs are classified as real or artificial. The distinguishing architecture is based on a convolutional neural network. It is not necessary to specify the input of the distinguishing section first, and here, the inputs can be considered as $N_x \times N_y \times N_c$. In this structure, $N_x \times N_y$ is the size of the images, which is 256 by 256, and N_c is the light intensity channel of the images used. In gray images, N_c is equal to one. The output that distinguishes a scalar number is zero and one, so it is considered binary and determines whether the image is real or fake. In most cases, a sigmoid activity function such as Equation (17) is used in the differentiating output. With the sigmoid function, the output can be normalized between zero and one:

$$f(x) = \frac{1}{1 + e^{-x}} \quad (17)$$

The following settings can be used for the differentiator in the proposed method:

• The zero layer, which is the input layer, has 256 by 256 input images.
• Hidden Layer 1: Uses 5 by 5 masks and 32 feature maps.
• Hidden Layer 2: Uses 5 by 5 size masks and uses 64 feature maps.
• Hidden Layer 3: Uses the full connection between Layers 2 and 3.
• Hidden Layer 4: Uses the full connection between Layers 3 and 4.

F. GENERATOR CLASSIFIER

The generator classifier unit uses a three-layer deconvolutional neural network. Its output is in the form of samples in the form $N_x \times N_y \times N_c$. The output also uses the activity function f (x) = tanh (x), which changes in the interval [−1, 1]. In this part of the GAN network, three layers are active as follows:

- Zero layers: input layer to receive noise vector
- Hidden layer one: this layer is connected to the zero layer and learns with masks of size 5 by 5 and a feature vector with 32 modes.
- The second hidden layer with 5 by 5 size masks and feature vector with 32 modes
- Output layer with outputs equal to 256 by 256, the size of the original image

The GAN deep learning network is based on game theory. A minimization and maximization game is performed by the manufacturer and the differentiator, respectively, as shown in Equation (18) [101]:

$$\min_{G} \max_{D} V(D, G) = E_{x_{P_{data}(x)}}[\log(D(x))]$$
$$+ E_{z_{P_z(z)}}[\log(1 - D(G(z)))] \quad (18)$$

In this regard, $p_{data}(x)$ are real training examples, and $E_{z_{P_z(z)}}$ are artificial training examples created using the noise process in images.

IV. EXPERIMENTAL RESULT

In this section, the implementation and results related to the analysis of the proposed method are discussed, and the test results are compared with several hand authentication methods.

A. DATASET

Two different databases are used to evaluate the methods proposed in this paper, the Jilin University - dorsal hand vein database [74] and the 11K Hands dataset [105]. The Jilin University - dorsal hand vein database contains several real images and many artificial images for the analysis and evaluation of biometric methods. The number of standard samples in this dataset is approximately 150 training images and 100 test images that can be used to teach the proposed method.

The 11K hands dataset is a set of 11,076 manual images (1, 600 × 1.200 pixels) of 190 subjects aged 18-75 years. Each individual was asked to open and close the fingers of his right and left hand, as it consisted of 5,680 images from the dorsal side, including 2,892 images for the right side and 2,788 images for the left hand, and 5,396 images on the palm, including 2,813 images for the palm print of the right palm and 2,583 images for the palm of the left palm. Each hand was depicted both dorsally and palmarly with a uniform white background and placed approximately the same distance from the camera. The suggested dataset contains a large number of manual images with more detailed metadata, as shown in Figure 8. The dataset is free for academic use.

B. EVALUATION CRITERIA

The proposed method is an authentication method and can be analyzed and evaluated with related indicators in this field. An indicator of the average accuracy of identification,
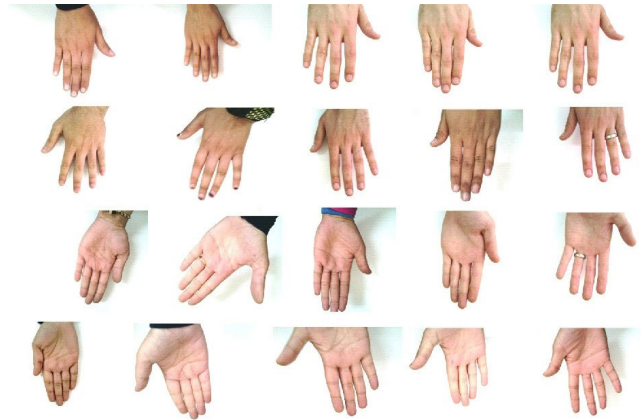

FIGURE 8. The 11K dataset.

the criterion of which is shown in Equation (19) [106]:

$$ACC_{Mean} = \frac{\sum_{i=1}^{Test} ACC_i}{Test} \quad (19)$$

where ACC_{Mean}, ACC_i, and Test are the average accuracy of authentication, accuracy in a test, and the number of tests, respectively. To calculate the accuracy of an experiment formulated with ACC_i, the number of matching modes can be divided by the total number of test specimens, and the accuracy of an experiment can be calculated according to Equation (20) [106]:

$$ACC_i = \frac{recognized\ images}{Total\ images} \quad (20)$$

The standard deviation in the experiments is also an important indicator of the evaluations. Reducing the standard deviation indicates more stability of the authentication algorithm. The standard deviation criterion is:

$$ACC_{std} = \sqrt{\frac{\sum_{i=1}^{Test}(ACC_i - ACC_{mean})^2}{Test}} \quad (21)$$

C. RESULTS AND DISCUSSION

To evaluate and implement the proposed method, we implemented it on two datasets. First, the results were analyzed on the Jilin University - dorsal hand vein database [74], and in the next section, the results are shown on the 11K hands dataset [105]. It can be diagnosed by similar methods, such as (LBP) [80], local phase quantization (LPQ) [83], Gabor [83], scale-invariant feature transform (SIFT) [86], flamelt-generated manifolds (FGM) [107] and biometric graph matching (BGM) [46]. Identity compared. There are three different thresholds for Otsu thresholds in the evaluations. The images are preprocessed before entering the GAN network, and the output results are compared with the desired methods.

Jilin University-Dorsal hand vein database results :

In Table 1, the proposed method is compared with the LBP, LPQ, GABOR, SIFT, FGM, and BGM methods in three indicators of accuracy (ACC), the standard deviation

TABLE 1. Comparison of accuracy (ACC), the standard deviation of the accuracy (STD), and equal error rate (EER).

Method	ACC	STD	EER
LBP	91.97	0.48	8.28
LPQ	92.33	0.43	8.17
GABOR	93.38	0.39	7.18
SIFT	96.69	0.21	3.92
FGM	94.03	0.30	5.56
BGM	95.47	0.29	9.89
DL-GAN	**98.36**	**0.192**	**2.47**

of accuracy (STD), and equal error rate (EER) in identifying individuals:

Experiments show that the proposed method is more efficient than DL-GAN, LBP, LPQ, GABOR, SIFT, FGM, and BGM in three indicators of accuracy, the standard deviation of accuracy and mean error in identifying individuals because it shows more accuracy. The proposed method has less error and standard deviation in experiments than the compared methods.
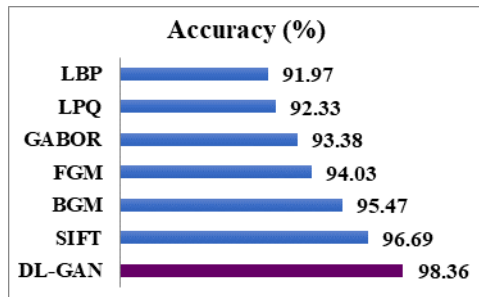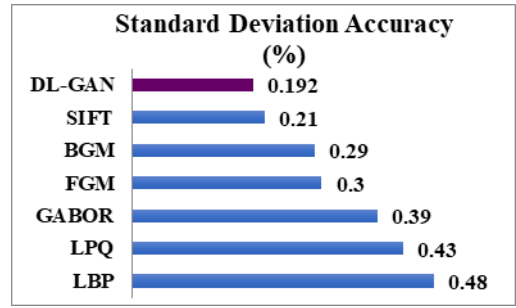

FIGURE 9. Comparing the accuracy of the proposed method with other learning methods. Change rates: 6.39 max%, 1.67 min%.

Fig. 9 shows a comparison of the accuracy index of the proposed method and other methods.
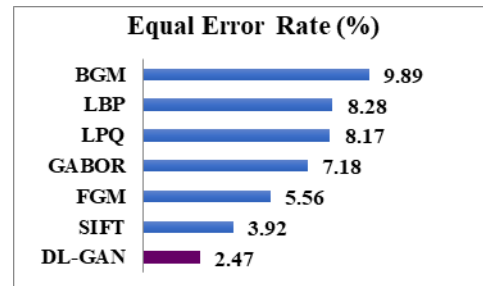
Experiments show the accuracy of the proposed method, LBP (91.97%), LPQ (92.33%), GABOR (93.38%), SIFT (96.69%), FGM (94.03%), BGM (95.47%) and DL-GAN (98.36%). The proposed method ranks first in the accuracy index, and the BGM method ranks second. The proposed method is approximately 1.67% more accurate than the SIFT method. The worst performance in these methods is related to the LBP method, which has an accuracy of approximately 91.97%.

As a show Figure 10. the proposed method is compared with other methods in the standard deviation index of accuracy and error, respectively. The standard deviation analysis shows that the standard deviation for identification in the proposed method, LBP(0.48), LPQ(0.43), GABOR(0.39), SIFT(0.21), FGM(0.3), BGM(0.29), and DL-GAN(0.192). The proposed method has the lowest standard deviation among the methods, which shows the greater stability of our proposed algorithm than other methods.

Fig. 11 shows the error of the proposed method, LBP(8.28), LPQ(8.17), GABOR (7.18), SIFT (3.92), FGM(5.56), BGM(9.89) and DL-GAN (2.47). The best performance is
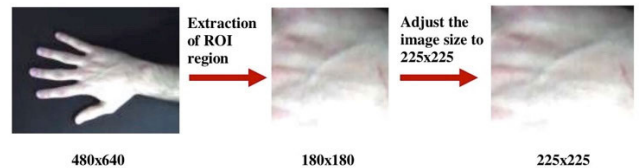

FIGURE 10. Comparison of the standard deviation of the proposed method with other learning methods. Change rates: 0.288 max%, 0.018 min%.

FIGURE 11. Comparing the error of the proposed method with other learning methods. Change rates:7.42 max%, 1,45 min%.

related to the proposed method, and the worst performance in the error index is related to the BGM method. Experiments show that the SIFT method has the lowest possible error compared to other methods after the proposed method.

FIGURE 12. Dorsal image preprocessing.

Figure 12. Comparing the error of the proposed method with other learning methods. Change rates:7.42 max%, 1,45 min%.

The 11K hands dataset [105] results.

Dorsal images have a rich texture and structural features, such as the mainline, wrinkles, triangles, and detail points. These features are unique and different for individuals. When collecting photos, images collected from the same fingerprints collected at different times will have different degrees of rotation and translation, and the size of the dorsal image collected may also differ simultaneously. Therefore, before extracting the feature and recognizing the dorsal image, it is necessary to extract the effective return on the investment area of the dorsal image that contains the main features. The entire treatment process is shown in Figure 12. Extracting the return on investment is a major step, and extracting the correct return on investment leads to image alignment, improved feature matching efficiency, and ultimately a positive impact on recognition results. Defining the region of interest (ROI) is

TABLE 2. Comparison of accuracy (ACC), the standard deviation of the accuracy (STD), and equal error rate (EER).

Method	ACC	STD	EER
LBP	92.86	0.41	8.42
LPQ	93.12	0.39	7.97
Gabor	94.21	0.37	7.23
SIFT	95.23	0.23	3.88
FGM	94.12	0.31	6.23
BGM	94.23	0.28	9.23
DL-GAN	**96.43**	**0.21**	**3.55**

TABLE 3. The experimental results of the DL-GAN method are seen according to the databases used.

	DATABASE					
	11K Database			Jilin Uni. Database		
METHOD	**ACC**	**STD**	**EER**	**ACC**	**STD**	**EER**
LBP	92.86	0.41	8.42	91.97	0.48	8.28
LPQ	93.12	0.39	7.97	92.33	0.43	8.17
GABOR	94.21	0.37	7.23	93.38	0.39	7.18
SIFT	95.23	0.23	3.88	96.69	0.21	3.92
FGM	94.12	0.31	6.23	94.04	0.30	5.56
BGM	94.23	0.28	9.23	95.47	0.29	9.89
DL-GAN	**96.43**	**0.21**	**3.55**	**98.36**	**0.19**	**2.47**

an essential step in biometric identification systems. For this, we used the same algorithm used in [108], [109] in our work. It consists of defining the coordinate system, which makes it possible to define the dorsal central area. As a result, there is a subimage of the H × W rectangular investment that is extracted afterward.

In Table 2, the proposed method based on the 11K hand dataset is compared with the LBP, LPQ, GABOR, SIFT, FGM, and BGM methods in three indicators of accuracy (ACC), the standard deviation of accuracy (STD), and equal error rate (EER) in identifying individuals:
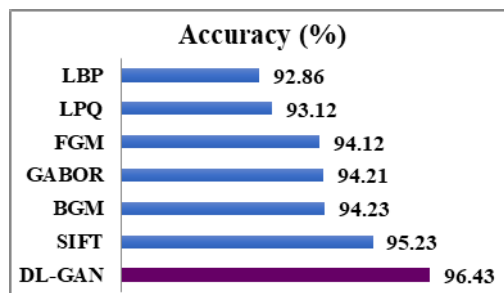
FIGURE 13. Comparing the accuracy of the proposed method with other learning methods. Change rates: 3.37 max%, 1,20 min%.
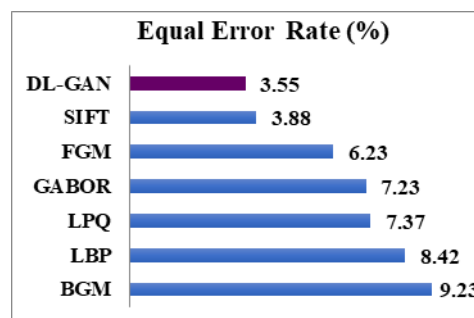
As shown in Figure 13, the experiments show that the accuracies of the proposed method are LBP (92.86%), LPQ (93.12%), GABOR (94.21%), SIFT (95.23%), FGM (94.12%), BGM (94.23%) and DL-GAN (96.43%). The proposed method ranks first in the accuracy index, and the SIFT method ranks second. The proposed method is approximately

1.20% more accurate than the BGM method. The worst performance in these methods is related to the LBP method, which has an accuracy of approximately 92.86%. A comparison of the accuracy index of the proposed method and other methods is shown in Figure 13:
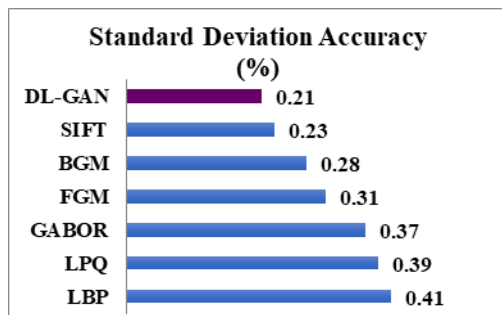
FIGURE 14. Comparison of the standard deviation of the proposed method with other learning methods. Change rates: 0,23 max%, 0,002 min%.

As shown in Figure 14, the proposed method is compared with other methods in the standard deviation index of accuracy and error. The standard deviation analysis shows the standard deviation for identification in the proposed method, LBP (0.41), LPQ (0.39), GABOR (0.37), SIFT (0.23), FGM (0.31), BGM (0.28) and DL-GAN (0.21). The proposed method has the lowest standard deviation among the methods, which shows the greater stability of our proposed algorithm than other methods.

FIGURE 15. Comparing the error of the proposed method with other learning methods. Change rates: 5.68 max%, 0.33 min%.

As shown in Figure 15, experiments show the error of the proposed method, LBP (8.42), LPQ (7.37), GABOR (7.23), SIFT (3.88), FGM (6.23), BGM (9.23) and DL-GAN (3.55). The best performance is related to the proposed method, and the worst performance in the error index is related to the BGM method. Experiments show that the SIFT method has the lowest possible error compared to other methods after the proposed method.

In this study, only two databases were used. There are many different methods and databases. Some of these are; Palmvein [110]–[112], putvein [113], dorsal hand-vein [114], [115], multispectral palmprint [116], [117], hand [118] and contactlesspalm [119] datasets and there are also new applications [120], [121].

V. CONCLUSION

In this study, a dorsal hand vein system was investigated to verify biometric identity. Deep learning and GAN were used together in the study. The advantage of deep learning is that we have made improvements for biometric identity verification trailer hand veins. The developed DL-GAN method has been tested in two databases. The experimental results obtained from Jilin University database experiment results show the accuracy of the proposed method, LBP (91.97%), LPQ (92.33%), GABOR (93.38%), SIFT (94.03%), FGM (96.69%), BGM (95.47%) and DL-GAN (98.36%). Rate of change: 6.39 max%, 1.67 min% were achieved. Experiments from the 11K dataset show that the accuracies of the proposed method are LBP (92.86%), LPQ (93.12%), GABOR (94.21%), SIFT (95.23%), FGM (94.12%), BGM (94.23%) and DL-GAN (96.43%). Rate of change: 3.37 max%, 1.20 min% have been achieved. We compare our results with LBP, LPQ, GABOR, SIFT, FGM, and BGM on the same benchmark using different experimental scenarios. The DL-GAN method achieves recognition rates when the discriminator size selected is 3, λ is 0.9000, and epsilon is 1.0000e-08. With these parameters, our method outperforms most of the others. The main reason is that the specific data for fine-tuning are limited. In addition, compared with handmade feature-based methods, deep generative adversarial network feature-based methods require little pre-processing and are more expedient to be applied in the real world. The advantage of the DL-GAN method is the use of a backhand structure for authentication, which increases its accuracy, and the main challenge of this method is the high complexity of the method. An important advantage of this method is that some of the dorsal parts may be lost due to damage, pigmentation or tattooing and affect the identity of individuals. This method has the advantage that it can create a large number of artificial samples for training to increase its accuracy and therefore will increase the power of this method for image classification. The disadvantage of DL-GAN is that it requires a large dataset, and preparing this dataset is not easy. With the distorted hand, it is difficult to identify. If the person loses a hand that time, it will impossible to recognize the person. The limitations of the DL-GAN method are that it requires considerable training data to achieve high accuracy.

REFERENCES

[1] F. Liu, G. Liu, Q. Zhao, and L. Shen, "Robust and high-security fingerprint recognition system using optical coherence tomography," *Neurocomputing*, vol. 402, pp. 14–28, Aug. 2020.

[2] M. Trokielewicz, A. Czajka, and P. Maciejewicz, "Post-mortem iris recognition with deep-learning-based image segmentation," *Image Vis. Comput.*, vol. 94, Feb. 2020, Art. no. 103866.

[3] L. Fei, B. Zhang, S. Teng, Z. Guo, S. Li, and W. Jia, "Joint multiview feature learning for hand-print recognition," *IEEE Trans. Instrum. Meas.*, vol. 69, no. 12, pp. 9743–9755, Dec. 2020.

[4] M. He, J. Zhang, S. Shan, M. Kan, and X. Chen, "Deformable face net for pose invariant face recognition," *Pattern Recognit.*, vol. 100, Apr. 2020, Art. no. 107113.

[5] Q. Abbas and M. E. A. Ibrahim, "DenseHyper: An automatic recognition system for detection of hypertensive retinopathy using dense features transform and deep-residual learning," *Multimedia Tools Appl.*, vol. 79, nos. 41–42, pp. 31595–31623, Nov. 2020.

[6] S. Veluchamy and L. R. Karlmarx, "HE-Co-HOG and k-SVM classifier for finger knuckle and palm print-based multimodal biometric recognition," *Sensor Rev.*, vol. 40, no. 2, pp. 203–216, May 2020.

[7] M. O. Oloyede, G. P. Hancke, and H. C. Myburgh, "A review on face recognition systems: Recent approaches and challenges," *Multimedia Tools Appl.*, vol. 79, nos. 37–38, pp. 27891–27922, Oct. 2020.

[8] A. R. Patil, A. D. Rahulkar, and C. N. Modi, "Designing an efficient fingerprint recognition system for infants and toddlers," in *Proc. 10th Int. Conf. Comput., Commun. Netw. Technol. (ICCCNT)*, Jul. 2019, pp. 1–7.

[9] W. Yang, S. Wang, J. Hu, G. Zheng, and C. Valli, "Security and accuracy of fingerprint-based biometrics: A review," *Symmetry*, vol. 11, no. 2, p. 141, Jan. 2019.

[10] C. Rathgeb, J. Wagner, and C. Busch, "SIFT-based iris recognition revisited: Prerequisites, advantages and improvements," *Pattern Anal. Appl.*, vol. 22, no. 3, pp. 889–906, Aug. 2019.

[11] N. Alay and H. H. Al-Baity, "Deep learning approach for multimodal biometric recognition system based on fusion of iris, face, and finger vein traits," *Sensors*, vol. 20, no. 19, p. 5523, Sep. 2020.

[12] Y. Pititheeraphab, N. Thongpance, H. Aoyama, and C. Pintavirooj, "Vein pattern verification and identification based on local geometric invariants constructed from minutia points and augmented with barcoded local feature," *Appl. Sci.*, vol. 10, no. 9, p. 3192, May 2020.

[13] A. Herbadji, Z. Akhtar, K. Siddique, N. Guermat, L. Ziet, M. Cheniti, and K. Muhammad, "Combining multiple biometric traits using asymmetric aggregation operators for improved person recognition," *Symmetry*, vol. 12, no. 3, p. 444, Mar. 2020.

[14] B. Hartung, D. Rauschning, H. Schwender, and S. Ritz-Timme, "A simple approach to use hand vein patterns as a tool for identification," *Forensic Sci. Int.*, vol. 307, Feb. 2020, Art. no. 110115.

[15] W. Nie, B. Zhang, and S. Zhao, "A novel hyperspectral based dorsal hand recognition system," in *Proc. 11th Int. Conf. Mach. Learn. Comput. (ICMLC)*, 2019, pp. 362–367.

[16] D. P. Wagh, H. S. Fadewar, and G. N. Shinde, "Biometric finger vein recognition methods for authentication," in *Computing in Engineering and Technology*. Singapore: Springer, 2020, pp. 45–53.

[17] K. Prihodova and M. Hub, "Biometric privacy through hand geometry— A survey," in *Proc. Int. Conf. Inf. Digit. Technol. (IDT)*, Jun. 2019, pp. 395–401.

[18] S. Barra, M. De Marsico, M. Nappi, F. Narducci, and D. Riccio, "A hand-based biometric system in visible light for mobile environments," *Inf. Sci.*, vol. 479, pp. 472–485, Apr. 2019.

[19] M. Klonowski, M. Plata, and P. Syga, "User authorization based on hand geometry without special equipment," *Pattern Recognit.*, vol. 73, pp. 189–201, Jan. 2018.

[20] J.-M. Guo, C.-H. Hsia, Y.-F. Liu, J.-C. Yu, M.-H. Chu, and T.-N. Le, "Contact-free hand geometry-based identification system," *Expert Syst. Appl.*, vol. 39, no. 14, pp. 11728–11736, Oct. 2012.

[21] P. Gupta, S. Srivastava, and P. Gupta, "An accurate infrared hand geometry and vein pattern based authentication system," *Knowl.-Based Syst.*, vol. 103, pp. 143–155, Jul. 2016.

[22] D. Zhong, H. Shao, and X. Du, "A hand-based multi-biometrics via deep hashing network and biometric graph matching," *IEEE Trans. Inf. Forensics Security*, vol. 14, no. 12, pp. 3140–3150, Dec. 2019.

[23] L. Fei, B. Zhang, Y. Xu, Z. Guo, J. Wen, and W. Jia, "Learning discriminant direction binary palmprint descriptor," *IEEE Trans. Image Process.*, vol. 28, no. 8, pp. 3808–3820, Aug. 2019.

[24] D. Zhong, X. Du, and K. Zhong, "Decade progress of palmprint recognition: A brief survey," *Neurocomputing*, vol. 328, pp. 16–28, Feb. 2019.

[25] W. Jia, B. Zhang, J. Lu, Y. Zhu, Y. Zhao, W. Zuo, and H. Ling, "Palmprint recognition based on complete direction representation," *IEEE Trans. Image Process.*, vol. 26, no. 9, pp. 4483–4498, Sep. 2017.

[26] L. Fei, G. Lu, W. Jia, S. Teng, and D. Zhang, "Feature extraction methods for palmprint recognition: A survey and evaluation," *IEEE Trans. Syst., Man, Cybern. Syst.*, vol. 49, no. 2, pp. 346–363, Feb. 2019.

[27] D. Zhong, H. Shao, and S. Liu, "Towards application of dorsal hand vein recognition under uncontrolled environment based on biometric graph matching," *IET Biometrics*, vol. 8, no. 2, pp. 159–167, Mar. 2019.

[28] Y. Wang, W. Xie, X. Yu, and L.-K. Shark, "An automatic physical access control system based on hand vein biometric identification," *IEEE Trans. Consum. Electron.*, vol. 61, no. 3, pp. 320–327, Aug. 2015.

[29] D. Huang, R. Zhang, Y. Yin, Y. Wang, and Y. Wang, "Local feature approach to dorsal hand vein recognition by centroid-based circular key-point grid and fine-grained matching," *Image Vis. Comput.*, vol. 58, pp. 266–277, Feb. 2017.

[30] W. Wu, S. J. Elliott, S. Lin, and W. Yuan, "Low-cost biometric recognition system based on NIR palm vein image," *IET Biometrics*, vol. 8, no. 3, pp. 206–214, May 2019.

[31] X. Yan, W. Kang, F. Deng, and Q. Wu, "Palm vein recognition based on multi-sampling and feature-level fusion," *Neurocomputing*, vol. 151, pp. 798–807, Mar. 2015.

[32] S. Ma, Z. Tao, X. Yang, Y. Yu, X. Zhou, and Z. Li, "Bathymetry retrieval from hyperspectral remote sensing data in optical-shallow water," *IEEE Trans. Geosci. Remote Sens.*, vol. 52, no. 2, pp. 1205–1212, Feb. 2014.

[33] W. Wang, Y. Fu, F. Dong, and F. Li, "Semantic segmentation of remote sensing ship image via a convolutional neural networks model," *IET Image Process.*, vol. 13, no. 6, pp. 1016–1022, May 2019.

[34] M. I. Lakhal, H. Çevikalp, S. Escalera, and F. Ofli, "Recurrent neural networks for remote sensing image classification," *IET Comput. Vis.*, vol. 12, no. 7, pp. 1040–1045, Oct. 2018.

[35] G. Chen, C. Li, and W. Sun, "Hyperspectral face recognition via feature extraction and CRC-based classifier," *IET Image Process.*, vol. 11, no. 4, pp. 266–272, Apr. 2017.

[36] M. A. Ferrer, A. Morales, and A. Díaz, "An approach to SWIR hyperspectral hand biometrics," *Inf. Sci.*, vol. 268, pp. 3–19, Jun. 2014.

[37] Z. Pan, G. Healey, M. Prasad, and B. Tromberg, "Face recognition in hyperspectral images," *IEEE Trans. Pattern Anal. Mach. Intell.*, vol. 25, no. 12, pp. 1552–1560, Dec. 2003.

[38] L. Wang and G. Leedham, "Near- and far-infrared imaging for vein pattern biometrics," in *Proc. IEEE Int. Conf. Video Signal Based Surveill.*, Sydney, NSW, Australia, Nov. 2006, p. 52.

[39] L. Fei, B. Zhang, W. Zhang, and S. Teng, "Local apparent and latent direction extraction for palmprint recognition," *Inf. Sci.*, vol. 473, pp. 59–72, Jan. 2019.

[40] D. Zhang, Z. Guo, G. Lu, L. Zhang, and W. Zuo, "An online system of multispectral palmprint verification," *IEEE Trans. Instrum. Meas.*, vol. 59, no. 2, pp. 480–490, Feb. 2010.

[41] D. Hong, W. Liu, J. Su, Z. Pan, and G. Wang, "A novel hierarchical approach for multispectral palmprint recognition," *Neurocomputing*, vol. 151, pp. 511–521, Mar. 2015.

[42] A. Rice. *A Quality Approach to Biometric Imaging*. Accessed: Oct. 6, 2019. [Online]. Available: https://ieeexplore.ieee.org/document/307921

[43] D. Huang, X. Zhu, Y. Wang, and D. Zhang, "Dorsal hand vein recognition via hierarchical combination of texture and shape clues," *Neurocomputing*, vol. 214, pp. 815–828, Nov. 2016.

[44] J. Wang, G. Wang, and M. Zhou, "Bimodal vein data mining via cross-selected-domain knowledge transfer," *IEEE Trans. Inf. Forensics Security*, vol. 13, no. 3, pp. 733–744, Mar. 2018.

[45] S.-J. Chuang, "Vein recognition based on minutiae features in the dorsal venous network of the hand," *Signal, Image Video Process.*, vol. 12, no. 3, pp. 573–581, Mar. 2018.

[46] K. Chen and D. Zhang, "Band selection for improvement of dorsal hand recognition," in *Proc. Int. Conf. Hand-Based Biometrics*, Hong Kong, Nov. 2011, pp. 1–4.

[47] X. Chen, Z. Zhou, J. Zhang, Z. Liu, and Q. Huang, "Local convex-and-concave pattern: An effective texture descriptor," *Inf. Sci.*, vol. 363, pp. 120–139, Oct. 2016.

[48] L. Liu, J. Chen, P. Fieguth, G. Zhao, R. Chellappa, and M. Pietikäinen, "From BoW to CNN: Two decades of texture representation for texture classification," *Int. J. Comput. Vis.*, vol. 127, no. 1, pp. 74–109, Jan. 2019.

[49] X. Wu, D. Zhang, and K. Wang, "Palm line extraction and matching for personal authentication," *IEEE Trans. Syst., Man, Cybern. A, Syst., Humans*, vol. 36, no. 5, pp. 978–987, Sep. 2006.

[50] D. Zhang, W.-K. Kong, J. You, and M. Wong, "Online palmprint identification," *IEEE Trans. Pattern Anal. Mach. Intell.*, vol. 25, no. 9, pp. 1041–1050, Sep. 2003.

[51] Y. Xu, L. Fei, J. Wen, and D. Zhang, "Discriminative and robust competitive code for palmprint recognition," *IEEE Trans. Syst., Man, Cybern. Syst.*, vol. 48, no. 2, pp. 232–241, Feb. 2018.

[52] Y. Wang, K. Zhang, and L. Shark, "Personal identification based on multiple keypoint sets of dorsal hand vein images," *IET Biometrics*, vol. 3, no. 4, pp. 234–245, Dec. 2014.

[53] J.-C. Lee, T.-M. Lo, and C.-P. Chang, "Dorsal hand vein recognition based on directional filter bank," *Signal, Image Video Process.*, vol. 10, no. 1, pp. 145–152, Jan. 2016.

[54] Z. Yao, J. Le Bars, C. Charrier, and C. Rosenberger, "Literature review of fingerprint quality assessment and its evaluation," *IET Biometrics*, vol. 5, no. 3, pp. 243–251, Sep. 2016.

[55] A. Abhyankar and S. Schuckers, "Iris quality assessment and bi-orthogonal wavelet based encoding for recognition," *Pattern Recognit.*, vol. 42, no. 9, pp. 1878–1894, Sep. 2009.

[56] A. Abaza, M. A. Harrison, T. Bourlai, and A. Ross, "Design and evaluation of photometric image quality measures for effective face recognition," *IET Biometrics*, vol. 3, no. 4, pp. 314–324, Dec. 2014.

[57] J. Wang and G. Wang, "Quality-specific hand vein recognition system," *IEEE Trans. Inf. Forensics Security*, vol. 12, no. 11, pp. 2599–2610, Nov. 2017.

[58] S. Shao, D. Zhou, R. He, J. Li, S. Zou, K. Mallery, S. Kumar, S. Yang, and J. Hong, "Risk assessment of airborne transmission of COVID-19 by asymptomatic individuals under different practical settings," *J. Aerosol Sci.*, vol. 151, Jan. 2021, Art. no. 105661.

[59] J. M. Cross and C. L. Smith, "Thermographic imaging of the subcutaneous vascular network of the back of the hand for biometric identification," in *Proc. Inst. Electr. Electron. Eng., 29th Annu. Int. Carnahan Conf. Secur. Technol.*, 1995, pp. 20–35.

[60] K. Wang, Y. Zhang, Z. Yuan, and D. Zhuang, "Hand vein recognition based on multi supplemental features of multi-classifier fusion decision," in *Proc. Int. Conf. Mechatronics Automat.*, Jun. 2006, pp. 1790–1795.

[61] C.-L. Lin and K.-C. Fan, "Biometric verification using thermal images of palm-dorsa vein patterns," *IEEE Trans. Circuits Syst. Video Technol.*, vol. 14, no. 2, pp. 199–213, Feb. 2004.

[62] A. Kumar and K. V. Prathyusha, "Personal authentication using hand vein triangulation and knuckle shape," *IEEE Trans. Image Process.*, vol. 18, no. 9, pp. 2127–2136, Sep. 2009.

[63] X. Zhu and D. Huang, "Hand dorsal vein recognition based on hierarchically structured texture and geometry features," in *Proc. Chin. Conf. Biometric Recognit.*, 2012, pp. 157–164.

[64] M. H.-M. Khan, R. K. Subramanian, and N. A. M. Khan, "Representation of hand dorsal vein features using a low dimensional representation integrating Cholesky decomposition," in *Proc. 2nd Int. Congr. Image Signal Process.*, 2009, pp. 1–6.

[65] M. H.-M. Khan and N. A. M. Khan, "Investigating linear discriminant analysis (LDA) on dorsal hand vein images," in *Proc. 3rd Int. Conf. Innov. Comput. Technol. (INTECH)*, Aug. 2013, pp. 54–59.

[66] Y. Wang, K. Li, J. Cui, L.-K. Shark, and M. Varley, "Study of hand-dorsa vein recognition," in *Proc. Int. Conf. Intell. Comput.*, 2010, pp. 490–498.

[67] D. Huang, Y. Tang, Y. Wang, L. Chen, and Y. Wang, "Hand vein recognition based on oriented gradient maps and local feature matching," in *Proc. Asian Conf. Comput. Vis.*, 2012, pp. 430–444.

[68] Y. Tang, D. Huang, and Y. Wang, "Hand-dorsa vein recognition based on multi-level keypoint detection and local feature matching," in *Proc. 21st Int. Conf. Pattern Recognit. (ICPR)*, 2012, pp. 2837–2840.

[69] D. Huang, Y. Tang, Y. Wang, L. Chen, and Y. Wang, "Hand-dorsa vein recognition by matching local features of multisource keypoints," *IEEE Trans. Cybern.*, vol. 45, no. 9, pp. 1823–1837, Sep. 2015.

[70] D. Huang, X. Zhu, Y. Wang, and D. Zhang, "Dorsal hand vein recognition via hierarchical combination of texture and shape clues," *Neurocomputing*, vol. 214, pp. 815–828, Nov. 2016.

[71] M. E. Cimen, O. F. Boyraz, M. Z. Yildiz, and A. F. Boz, "A new dorsal hand vein authentication system based on fractal dimension box counting method," *Optik*, vol. 226, Jan. 2021, Art. no. 165438.

[72] Y. Aberni, L. Boubchir, and B. Daachi, "Palm vein recognition based on competitive coding scheme using multi-scale local binary pattern with ant colony optimization," *Pattern Recognit. Lett.*, vol. 136, pp. 101–110, Aug. 2020.

[73] O. Alpar, "A novel fuzzy curvature method for recognition of anterior forearm subcutaneous veins by thermal imaging," *Expert Syst. Appl.*, vol. 120, pp. 33–42, Apr. 2019.

[74] F. Liu, S. Jiang, B. Kang, and T. Hou, "A recognition system for partially occluded dorsal hand vein using improved biometric graph matching," *IEEE Access*, vol. 8, pp. 74525–74534, 2020.

[75] A. Achban, H. A. Nugroho, and P. Nugroho, "Wrist hand vein recognition using local line binary pattern (LLBP)," in *Proc. 5th Int. Conf. Sci. Technol. (ICST)*, vol. 1, Jul. 2019, pp. 1–6.

[76] H. Qin, M. A. El Yacoubi, J. Lin, and B. Liu, "An iterative deep neural network for hand-vein verification," *IEEE Access*, vol. 7, pp. 34823–34837, 2019.

[77] R. Garcia-Martin and R. Sanchez-Reillo, "Vein biometric recognition on a smartphone," *IEEE Access*, vol. 8, pp. 104801–104813, 2020.

[78] R. S. Kuzu, E. Piciucco, E. Maiorana, and P. Campisi, "On-the-fly finger-vein-based biometric recognition using deep neural networks," *IEEE Trans. Inf. Forensics Security*, vol. 15, pp. 2641–2654, 2020.

[79] X. Li, D. Huang, R. Zhang, Y. Wang, and X. Xie, "Hand dorsal vein recognition by matching width skeleton models," in *Proc. IEEE Int. Conf. Image Process. (ICIP)*, Sep. 2016, pp. 3146–3150.

[80] K. Li, G. Zhang, Y. Wang, P. Wang, and C. Ni, "Hand-dorsa vein recognition based on improved partition local binary patterns," in *Proc. Chin. Conf. Biometric Recognit.*, 2015, pp. 312–320.

[81] W. Kang and Q. Wu, "Contactless palm vein recognition using a mutual foreground-based local binary pattern," *IEEE Trans. Inf. Forensics Security*, vol. 9, no. 11, pp. 1974–1985, Nov. 2014.

[82] Y. Wang, Q. Duan, L.-K. Shark, and D. Huang, "Improving hand vein recognition by score weighted fusion of wavelet-domain multi-radius local binary patterns," *Int. J. Comput. Appl. Technol.*, vol. 54, no. 3, pp. 151–160, 2016.

[83] K. Premalatha and A. M. Natarajan, "Hand vein pattern recognition using natural image statistics," *Def. Sci. J.*, vol. 65, no. 2, p. 150, 2015.

[84] K. Premalatha and A. M. Natarajan, "A dorsal hand vein recognition-based on local Gabor phase quantization with whitening transformation," *Def. Sci. J.*, vol. 64, no. 2, p. 159, 2014.

[85] W. Nie, B. Zhang, and S. Zhao, "Discriminative local feature for hyperspectral hand biometrics by adjusting image acutance," *Appl. Sci.*, vol. 9, no. 19, p. 4178, Oct. 2019.

[86] Y. Wang and X. Zheng, "Cross-device hand vein recognition based on improved SIFT," *Int. J. Wavelets, Multiresolution Inf. Process.*, vol. 16, no. 02, Mar. 2018, Art. no. 1840010.

[87] R. Wang, G. Wang, Z. Chen, Z. Zeng, and Y. Wang, "A palm vein identification system based on Gabor wavelet features," *Neural Comput. Appl.*, vol. 24, no. 1, pp. 161–168, Jan. 2014.

[88] Z. Meng and X. Gu, "Hand vein identification using local Gabor ordinal measure," *J. Electron. Imag.*, vol. 23, no. 5, p. 53004, 2014.

[89] A. B. J. Teoh and L. Leng, "Special issue on advanced biometrics with deep learning," *Appl. Sci.*, vol. 10, no. 13, p. 4453, Jun. 2020.

[90] Y. LeCun, Y. Bengio, and G. Hinton, "Deep learning," *Nature*, vol. 521, pp. 436–444, May 2015.

[91] N. Al-Johania and L. Elrefaei, "Dorsal hand vein recognition by convolutional neural networks: Feature learning and transfer learning approaches," *Int. J. Intell. Eng. Syst.*, vol. 12, no. 3, pp. 178–191, Jun. 2019.

[92] Y. LeCun, Y. Bengio, and G. Hinton, "Deep learning," *Nature*, vol. 521, pp. 436–444, May 2015.

[93] N. C. Thompson, K. Greenewald, K. Lee, and G. F. Manso, "The computational limits of deep learning," Jul. 2020, *arXiv:2007.05558*. [Online]. Available: https://arxiv.org/abs/2007.05558

[94] I. Goodfellow, Y. Bengio, and A. Courville, *Deep Learning*. Cambridge, MA, USA: MIT Press, 2017.

[95] J. D. Kelleher, *Deep Learning*. Cambridge, MA, USA: MIT Press, 2019.

[96] S. Minaee, A. Abdolrashidi, H. Su, M. Bennamoun, and D. Zhang, "Biometric recognition using deep learning: A survey," 2019, *arXiv:1912.00271*. [Online]. Available: https://arxiv.org/abs/1912.00271

[97] I. J. Goodfellow, J. Pouget-Abadie, M. Mirza, B. Xu, D. Warde-Farley, S. Ozair, A. Courville, and Y. Bengio, "Generative adversarial networks," 2014, *arXiv:1406.2661*. [Online]. Available: https://arxiv.org/abs/1406.2661

[98] Z. Wang, Q. She, and T. E. Ward, "Generative adversarial networks in computer vision: A survey and taxonomy," 2019, *arXiv:1906.01529*. [Online]. Available: http://arxiv.org/abs/1906.01529

[99] S. I. T. Joseph, J. Sasikala, and D. S. Juliet, "Detection of ship from satellite images using deep convolutional neural networks with improved median filter," in *Artificial Intelligence Techniques for Satellite Image Analysis*. Cham, Switzerland: Springer, 2020, pp. 69–82.

[100] B. Küçükuğurlu and E. Gedikli, "Symbiotic organisms search algorithm for multilevel thresholding of images," *Expert Syst. Appl.*, vol. 147, Jun. 2020, Art. no. 113210.

[101] I. J. Goodfellow, J. Pouget-Abadie, M. Mirza, B. Xu, D. Warde-Farley, S. Ozair, A. C. Courville, and Y. Bengio, "Generative adversarial nets," in *Proc. Adv. Neural Inf. Process. Syst.*, 2014, pp. 2672–2680.

[102] M. Mirza and S. Osindero, "Conditional generative adversarial nets," 2014, *arXiv:1411.1784*. [Online]. Available: http://arxiv.org/abs/1411.1784

[103] A. Odena, C. Olah, and J. Shlens, "Conditional image synthesis with auxiliary classifier GANs," in *Proc. Int. Conf. Mach. Learn.*, 2017, pp. 2642–2651.

[104] G. Jha and H. Cecotti, "Data augmentation for handwritten digit recognition using generative adversarial networks," *Multimedia Tools Appl.*, vol. 79, pp. 1–14, Dec. 2020.

[105] M. Afifi, "11K hands: Gender recognition and biometric identification using a large dataset of hand images," *Multimedia Tools Appl.*, vol. 78, no. 15, pp. 20835–20854, Aug. 2019.

[106] R. B. Trabelsi, A. D. Masmoudi, and D. S. Masmoudi, "Hand vein recognition system with circular difference and statistical directional patterns based on an artificial neural network," *Multimedia Tools Appl.*, vol. 75, no. 2, pp. 687–707, Jan. 2016.

[107] S. M. Lajevardi, A. Arakala, S. Davis, and K. J. Horadam, "Hand vein authentication using biometric graph matching," *IET Biometrics*, vol. 3, no. 4, pp. 302–313, Dec. 2014.

[108] A. S. Al-Waisy, R. Qahwaji, S. Ipson, S. Al-Fahdawi, and T. A. M. Nagem, "A multi-biometric iris recognition system based on a deep learning approach," *Pattern Anal. Appl.*, vol. 21, no. 3, pp. 783–802, Aug. 2018.

[109] A. S. Al-Waisy, R. Qahwaji, S. Ipson, and S. Al-Fahdawi, "A multi-modal biometrie system for personal identification based on deep learning approaches," in *Proc. 7th Int. Conf. Emerg. Secur. Technol. (EST)*, Sep. 2017, pp. 163–168.

[110] *VERA PalmVein*. Accessed: Apr. 10, 2021. [Online]. Available: https://www.idiap.ch/dataset/vera-palmvein

[111] *Palm Vein Data Base*. Accessed: Apr. 10, 2021. [Online]. Available: https://biometrics.put.poznan.pl/vein-dataset

[112] *The Palmvein Recognition Library*. Accessed: Apr. 10, 2021. [Online]. Available: https://pypi.org/project/bob.palmvein/

[113] [Online]. Available: https://pythonhosted.org/bob.db.putvein/

[114] [Online]. Available: https://www.kaggle.com/oboyraz/suas-dorsal- hand-vein-database Data SUAS Dorsal Hand Vein Database

[115] *Hand-Dorsa-Vein-Dataset*. Accessed: Apr. 12, 2021. [Online]. Available: https://github.com/Multimedia-Lab-CUMT/Hand-dorsa-Vein-Dataset

[116] *Casia Multi Spectral Palmprint V1 Database*. Accessed: Apr. 12, 2021. [Online]. Available: http://biometrics.idealtest.org/ dbDetailForUser.do?id=6

[117] *Polyu Multi Spectral Palmprint Database*. Accessed: Apr. 12, 2021. [Online]. Available: http://www4.comp.polyu.edu.hk/?biometrics/MultispectralPalmprint/MSP.htm

[118] *Bosphorus Hand Database*. Accessed: Apr. 11, 2021. [Online]. Available: http://bosphorus.ee.boun.edu.tr/hand/Home.aspx

[119] *Towards Contactless Palmprint Recognition: A Novel Device, A New Benchmark, and A Collaborative Representation Based Identification Approach*. Accessed: Apr. 11, 2021. [Online]. Available: http://sse.tongji.edu.cn/linzhang/contactlesspalm/ index.htm

[120] Ö. Toygar, F. O. Babalola, and Y. Bitirim, "FYO: A novel multimodal vein database with palmar, dorsal and wrist biometrics," *IEEE Access*, vol. 8, pp. 82461–82470, Apr. 2020, doi: 10.1109/ACCESS.2020.2991475.

[121] A. Yuksel, L. Akarun, and B. Sankur, "Biometric identification through hand vein patterns," in *Proc. Int. Workshop Emerg. Techn. Challenges Hand-Based Biometrics*, Istanbul, Turkey, Aug. 2010, pp. 1–6, doi: 10.1109/ETCHB.2010.5559295.

KHALED MOHAMED ALASHIK received the B.S. degree in electric engineering from the Engineering Academy Tajoura, Tripoli, Libya, in 1996, and the Master of Engineering degree in communication and computer from the University Kebangsaan Malaysia (UKM), Bangi, Malaysia, in 2007. He is currently pursuing the Ph.D. degree in computer engineering with Ankara Yildirim Beyazit University, Ankara, Turkey. From 2008 to 2016, he was with the Research Center, Tripoli, Libya. His research interests include computer vision and machine learning, especially biometrics.

REMZI YILDIRIM received the B.S. and M.S. degrees in electronics and computer engineering from Gazi University, Ankara, Turkey, in 1988 and 1993, respectively, and the Ph.D. degree in electronics from Erciyes University, Kayseri, Turkey, in 1996. From 1999 to 2002, he was a Visiting Scholar with the Massachusetts Institute of Technology, Boston, MA, USA. From 2004 to 2005, he was a Visiting Scholar with Liverpool University, Liverpool, U.K. He is currently a Professor with the Department of Computer Engineering, Ankara Yildirim Beyazit University, Ankara. He has published more than 100 journal articles and conference papers and 21 books. His research interests include optoelectronics, cyber physical systems, and model checking.

• • •